

## DETECTION AND CHARACTERIZATION OF B-STAGED ADHESIVE MATERIAL VARIABILITY THROUGH QUANTITATIVE TACKINESS EVALUATION

Marty Lorgino D. Pulutan

Jelvic D. Fundan

Maria Sandra T. Brucelo

Backend Technologies

Ampleon Philippines, Inc., Light Industry & Science Park I, Brgy. Diezmo, Cabuyao City, Laguna

marty.lorgino.pulutan@ampleon.com

### ABSTRACT

The study proposes a quantitative tackiness measurement of B-staged capsealing glue as an effective method of monitoring the material's rheological variability which causes Gross Leak Test (GLT) failures reaching up to 20%. Through defect mapping, B-stage rheological characterization, Tackiness Test and Design of Experiments (DoE), the researchers determined the contributors to the capsealing glue defect. Results reveal that defects such as pinholes, insufficient flow, and stretched glue are highly attributed to adhesive flow dynamics and cure kinetics of the B-staged material. Rheological characterization revealed that the B-staged epoxy requires precise timing within the  $\alpha$ - and  $\beta$ -phase transitions for void mitigation and interface integrity. An optimized process parameter window defined from the DoE is recommended – load time of approximately 80 seconds, vacuum-off at around 100 seconds and a minimum cure cycle duration of 900 seconds. To address persistent material variability, real-time Tackiness Testing was adopted as a proactive control strategy enabling timely adjustments in capsealing parameters. Implementation of the monitoring protocol effectively reduced defect incidence, stabilized GLT yields and enhanced capsealing process resilience. The findings underscore the importance of integrating thermal-rheological material behavior with mechanical precision to ensure hermetic reliability in ACC packages.

### 1.0 INTRODUCTION

The Air Cavity Ceramic (ACC) package has long been established as a preferred packaging architecture in the RF power industry particularly for encapsulating sensitive components such as GaN dies. The hermeticity and low parasitic characteristics make it the package of choice for a wide spectrum of devices for non-cellular communication systems applications including industrial, scientific, and medical (ISM) transmitters, radar systems, and broadcast equipment. The ceramic-based structure of the ACC comprises a ceramic ringframe and lid, provides an effective electromagnetic shield while ensuring mechanical protection and environmental isolation of sensitive components.

For years, the production of ACC devices has demonstrated consistency in both process reliability and product yield, reflecting the maturity and robustness of the existing assembly flow. However, recent records over the past year have revealed an alarming increase in GLT failures with rejection rates surging to as high as 20% as shown in Fig. 1. The spike represents a significant deviation from historical performance baselines and poses a considerable threat to overall production efficiency and cost-effectiveness.



Fig. 1. Percentage of GLT Rejects by Month Closed With Trendline Overlay.

Initial root cause analyses backed by early-stage failure investigation data, strongly implicate poor adhesion between the ceramic lid and the ceramic ringframe as the primary contributor to the formation of voids or delamination at the bonding interface. The interfacial defects act as leakage paths that compromise the hermetic seal of the package leading to bubble leaks and eventual GLT failures. The observed degradation in adhesion performance suggests that subtle changes either in material properties, process parameters or the machine condition used during capsealing may be the factor affecting the reliability of the lid-to-ringframe joint.

Given the critical function of hermeticity in maintaining long-term device performance and reliability particularly in RF power devices operating in stringent and high-power environments, the issue demands an in-depth analysis and concrete detection of root cause. The present study aims to systematically evaluate the factors influencing ceramic-to-ceramic adhesion in ACC packages, identify the root causes of GLT anomalies and propose material-level variability

detection that could be basis for capsealing process optimization.

## 2. 0 REVIEW OF RELATED WORK

Several existing studies have dealt with characterization of adhesives and epoxy resins to enhance material performance and process workability. The study conducted by Joy et al. assumes that poor miscibility triggers formation of microvoids or weak interfaces within the glue which acts as pathways for leakage when subjected under thermal or pressure stress<sup>1</sup>. A related study by Müller-Pabel et al. emphasized the pivotal role of viscoelastic properties in determining the performance of thermosetting materials which could be related to capsealing process of pre-glued B-staged ceramic. The properties which are characterized by the time- and temperature-dependent response of modulus, creep, and stress relaxation, are governed by the interplay between elastic and viscous deformation mechanisms, which in turn are influenced by the polymer's molecular structure and network topology<sup>2</sup>. In the context of B-stage adhesives, the preservation of chain mobility enables the self-healing of microdefects incurred due to thermal or mechanical perturbations including outgassing. The authors also highlight the use of advanced characterization techniques including dynamic mechanical analysis (DMA) and rheometer to monitor the evolution of viscoelastic behavior throughout the curing process<sup>2</sup>. However, acquiring such equipment may pose a significant financial burden for companies that have yet to invest in it particularly given that many corporate strategic initiatives are predominantly focused on cost reduction. Moreover, Bourchak et al. showed that preheating enhances resin flow and wetting and reduces void formation at the die or package interface while post-curing enhances the cross-link density which directly improve mechanical strength and barrier performance. Insufficient post-curing may leave the material susceptible to delamination leading to leakage<sup>3</sup>.

Among all resin systems, B-stage is commonly employed in the capsealing process for its tack-free handling and ability to cure later during package assembly. Measuring the degree of cure ( $\alpha$ ) during the B-stage ensures optimal processing and performance and guarantees reliability<sup>4</sup>. In the study done by Appelt and Cook, Differential Scanning Calorimetry (DSC) was used to measure the heat of reaction during curing. The degree of cure ( $\alpha$ ) was calculated using the equation,

$$\alpha = \frac{\Delta H_t}{\Delta H_{TOTAL}} \quad (\text{Equation 1})$$

where  $\Delta H_t$  is the partial heat of reaction at time  $t$  and  $\Delta H_{TOTAL}$  is the total heat of reaction for full cure<sup>5</sup>. Tracking the degree of cure allows control of the B-staging process to prevent premature curing or undercuring both of which compromise

seal integrity. Additionally, Liu et al. developed a mathematical model to predict the cure progression under varying temperature-time profiles. The approach allows a more accurate characterization of B-stage epoxy during late-stage curing particularly at high temperatures and is instrumental in simulating the curing behavior of B-stage materials used in electronics packaging<sup>6</sup>.

Collectively, the cited studies highlight the dependence of epoxy resin performance on compositional, kinetic, and thermal parameters. Ensuring leak-tight encapsulation demands a holistic approach that integrates materials compatibility, thermoset kinetics and process thermodynamics to optimize the capsealing process and entails concrete material variability detection to optimize process parameters accordingly.

## 3.0 METHODOLOGY

### 4.1 Defect Mapping and Classification

All GLT-failed units were inspected using a 15 $\times$  optical microscope to identify defect types, origins and locations. Defects were mapped spatially as shown in Fig. 2 with frequency annotations per region. Three primary failure types were identified – pinholes, insufficient flow and stretched glue as exhibited in Fig. 3.

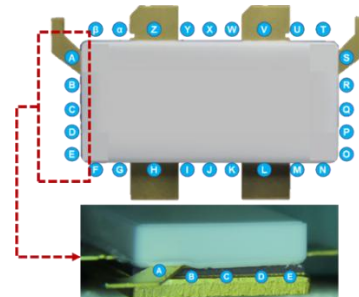


Fig. 2. Defect Mapping Using Annotation per Area Along Unit Perimeter.

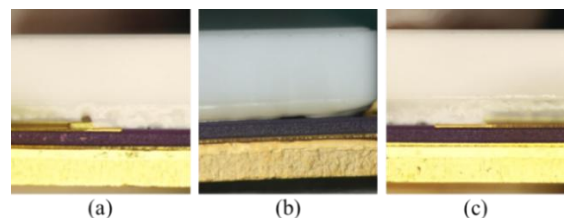


Fig. 3. Defect Signatures Showing (a) Pinhole, (b) Insufficient Flow and (c) Stretched Glue.

### 4.2 Cap Placement and Tilt Evaluation

Cap placement deviations along the right, left, top, and bottom edges relative to the ringframe were quantified using a video measurement system. The measured deviations were

subsequently plotted as a histogram to evaluate conformity with the nominal placement specifications.

#### 4.3 Tackiness Testing and Gelation Profiling

Tackiness testing was conducted by subjecting three samples of each ceramic cap per batch to an isothermal condition of  $180 \pm 5^\circ\text{C}$  to characterize adhesive behavior across gelation phases ( $\alpha$ ,  $\beta$ ,  $\gamma$ ). A tungsten wire was used to periodically probe the B-staged adhesive at 10-second intervals during hot plate exposure with the material response categorized as soft, rubbery, or hard (see Fig. 13 in the Appendix for reference). The material response from 0 seconds (when the cap is immediately placed on the hot plate) and every 10 seconds until it fully hardens, are recorded.

#### 4.4 Process Optimization via DoE

A Full Factorial Design of Experiments (DoE) consisting of 6 experimental legs was utilized to evaluate the effects of load time (LT) and vacuum-off (VO) settings with factor levels derived from the Tackiness Test. For each parameter combination, 30 units were assembled to ensure sufficient sampling for normal distribution assumptions. The measured responses included GLT yield per run and cap shear strength. Response Surface Analysis (RSA) was used to identify the optimal process parameters based on the obtained responses.

## 4.0 RESULTS AND DISCUSSION

#### 4.2 Defect Mapping

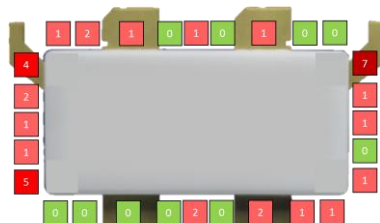


Fig. 4. Defect Mapping of Pinhole Defects.

Figure 4 illustrates the spatial distribution of units presenting pinhole defects characterized by the defect morphology depicted in Figure 3. A pronounced clustering of pinhole occurrences is observed at the corners of the units which implies that unit corners act as mechanical stress concentrators and preferential sites for pressure relief. During the gelation phase as crosslinking progresses, the viscosity of glue rises sharply, trapping any residual volatiles or entrapped air within the adhesive matrix. The resulting internal pressure gradients seek the path of least resistance, leading to breach events at the structurally weaker corners where mechanical constraint is reduced. Once the localized

pressure exceeds the cohesive strength of the partially cured adhesive, pinholes are formed as the system approaches mechanical equilibrium.



Fig. 5. Defect Mapping of Insufficient Flow Defects.

The second type of defect termed *insufficient flow* is defined by regions where the cured glue demonstrates inadequate coverage onto the ceramic substrate. Microscopic inspection reveals that such defects predominantly occur along the peripheral edges of the units with a higher concentration along the shorter sides. Detailed defect mapping and spatial analysis suggest that the material advanced toward its gel point abruptly without completely interlocking with the ceramic ringframe. At this stage, the ability of glue to properly wet and conform to the surface topography of the ceramic ringframe diminishes which consequently produces weak adhesion zones. The compromised interfacial regions act as preferential sites for pressure leakage during subsequent capsealing operations as the weak adhesive bond cannot withstand the internal pressure gradients generated during capsealing. Such observations highlight the importance of precisely timing the bonding of pre-glued caps to the ceramic ringframe at the point where viscosity is at lowest.

The third glue defect, termed *stretched glue* (Fig. 14, Appendix), is marked by bondline elongation and surface wrinkling resulting from insufficient compressive force during cap-to-ceramic bonding, leading to poor adhesive flow and substrate wetting. Subsequent capsealing introduces tensile stress in these weak regions, causing deformation. Rheological data indicate that delayed engagement of caps beyond the adhesive's gel point—identified by a sharp rise in storage modulus ( $G'$ )—shifts the material into an elastic-dominant state, reducing flowability which promotes surface distortion and fracture within the partially cured network. The defect's spatial bias suggests mechanical nonuniformities in the Isothermal Sealing (ITS) platform, such as improper leveling or asymmetric force application, resulting in uneven contact pressure and localized defect zones.

Addressing such defect types require comprehensive optimization of the adhesive working window, precise synchronization of piston actuation within the low-viscosity phase, and mechanical calibration of the ITS machine to ensure uniform force distribution across all units

### 4.3 Quick Wins

#### 4.3.1 Placement of Cap with Respect to Ringframe

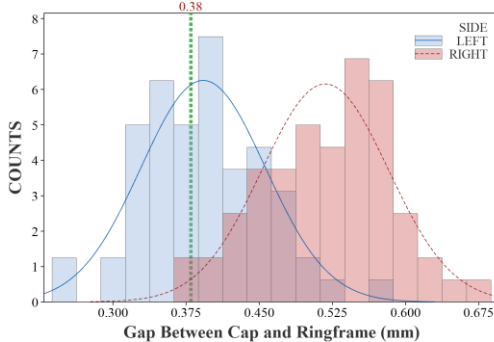


Fig. 6. Histogram of Cap Placement with Respect to Ringframe as Measured on Left and Right of the GLT Defective Samples.

The placement analysis as shown in Fig. 6, indicates that the cap is displaced from its nominal position along both the x- and y-axes. A leftward shift is observed on the x-axis, with a skew of -0.1253 mm while a downward shift on the y-axis is evidenced by a deviation of -0.14049 mm. The displacements correspond to increased gaps between the cap edges and the ringframe. Cap coplanarity was also assessed via tilt measurements along the z-axis, as illustrated in Fig. 7.

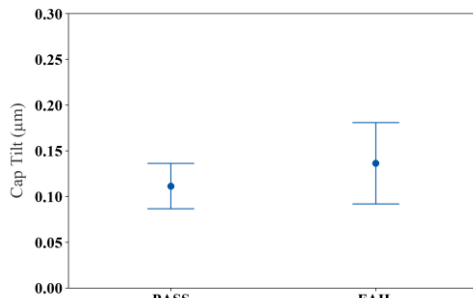


Fig. 7. Cap Tilt Distribution of Passed and Failed Units in GLT.

Cap tilt measurements were performed on all GLT-failed units and compared with representative passing units using a two-sample t-test under equal variance assumptions. No statistically significant difference in tilt—defined by the delta between the highest and lowest of the four corner points—was found suggesting minimal practical impact to GLT failures. However, the mean tilt of 0.115  $\mu$ m suggests that ITS plate recalibration may still be warranted for enhanced alignment control.

Following rework and alignment of the ITS machine, cap placement skewness values were reduced to 0.09, 0.11, 0.13, and 0.08 (top, bottom, left, right, respectively). Average positional offsets were -0.00392 mm (x-axis) and -0.00410 mm (y-axis), both within machine tolerances. The

adjustments effectively minimized placement deviations below the thresholds associated with GLT failure.

### 4.4 Material Characterization Through Tackiness Test

#### 4.4.1 Thermal Analysis of B-staged Epoxy

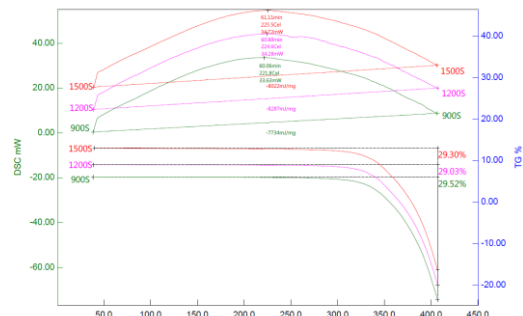


Fig. 8. DSC-TGA Plots of B-staged Epoxy Post Cured at 900, 1200 and 1500 seconds.

B-staged epoxy samples from pre-glued ceramic caps were initially subjected to dynamic heating following the supplier-recommended cure profile, followed by isothermal scans at 180 °C to simulate the full curing cycle of the ACC package. Results indicated that samples heated continuously for 900, 1200, and 1500 seconds achieved comparable degrees of cure calculated using Equation 1, suggesting that complete cross-linking likely occurred within the shortest duration of 900 seconds, rendering further extension of cure time negligible in effect.

#### 4.4.2 Tackiness Test

Utilizing the established methodology for quantifying the tackiness of B-staged adhesive as detailed in Section 3.0, tackiness test was systematically performed to obtain quantitative insights into the gelation kinetics of the glue under isothermal capsealing conditions at 180  $\pm$  5 °C. The corresponding phase transitions as a function of exposure time were determined and mapped to the gelation curve as shown in Fig. 9.

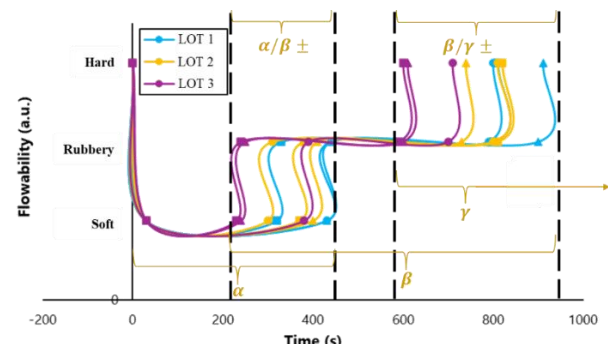


Fig. 9. Flowability Versus Time of B-Staged Cap Samples Randomly Obtained From Three Different Lots.

The B-staged cap glue undergo a significant reduction in viscosity, entering the  $\alpha$ -phase characterized by enhanced molecular mobility upon exposure to capsealing temperature<sup>2</sup>. At this phase, the glue flows onto the ceramic ringframe to initiate mechanical interlocking. Results have demonstrated that the viscosity decreases with increasing temperature, reaching a minimum before the onset of gelation that is within 200 to 400 seconds mark based on the plateau points on all samples tested. Such behavior underscores the importance of precisely timing the vacuum-off process during the low-viscosity window to ensure adequate adhesive spread and substrate wetting.

Progression into the  $\beta$ -phase signifies the onset of gelation, where the epoxy system transitions from a viscous liquid to a viscoelastic solid and loses the ability to flow. The phase transition is marked by the crossover point in dynamic rheological measurements where the storage modulus ( $G$ ) equals the loss modulus ( $G''$ ) indicating the formation of a cross-linked network<sup>2</sup>. Initiating vacuum-off beyond this point can impede proper adhesion due to insufficient wetting of the substrate<sup>1</sup>. As such vacuum off should be timed before the inferred onset of gelation point.

Subsequently, the system enters the  $\gamma$ -phase characterized by vitrification and the completion of curing through extensive cross-linking and network formation.<sup>2,3</sup> A minimum cycle time of 900 seconds is required to ensure attainment of the maximum vitrification point and complete cross-linking. Although extended cycle durations are permissible, the cycle time must be carefully balanced against throughput limitations dictated by units per hour (UPH) performance metrics.

On the other hand, material variability represented by  $\alpha+\beta-$  reflects shifts in the viscosity profile and gelation kinetics of the epoxy system<sup>1</sup> which impacts the loading time and vacuum-off settings. Insufficient loading time may leave residual solvents and absorbed moisture resulting in elevated internal cavity pressures while premature vacuum-off can cause uncontrolled glue flow out. Conversely, excessive delays lead to poor adhesion due to early gelation<sup>2</sup>. In the plot, the transition phase notably exhibits an overlap of approximately 250 seconds with the  $\beta$ -phase, which is indicative of gel point variability within the B-staged adhesive matrix. To facilitate adequate volatile outgassing while maintaining sufficient adhesive flow for optimal surface wetting, the load time must be initiated well before the earliest onset of gelation—preferably within the first 100 seconds of thermal exposure while the timing for vacuum-off should precede the 400-second mark. Based on the observed rheological profiles, the optimal vacuum-off window is identified between 100 and 300 seconds. Such recommended timing strategy prevents premature vacuum release which could otherwise result in excessive epoxy bleed-out.

Moreover,  $\beta+\gamma-$  variability indicates shifts in the vitrification point, establishing the minimum thermal exposure duration necessary to achieve a high degree of cure and ensure reliable bonding at the glue-to-ringframe interface<sup>2,3</sup>. Post-curing processes involving elevated temperatures can further enhance the cross-linking density and mechanical properties of the adhesive bond<sup>3</sup>. The observed temporal overlap between the  $\beta$ - and  $\gamma$ -phase transitions is associated with variation in the vitrification point of the adhesive system and should be used as the basis for determining the total cycle duration. Accordingly, a minimum of 900 seconds should be utilized to ensure complete crosslinking.

Building upon the inferences derived from the tackiness evolution curves, a Design of Experiments (DoE) was executed utilizing experimental legs defined from the Tackiness Test results with the objective of identifying optimal capsealing parameters capable of eliminating GLT failures.

#### 4.5 Optimization of Capsealing Parameters Through Design of Experiments

Six experimental legs, each incorporating variations in key capsealing parameters namely load time (LT) and vacuum-off timing (VO) were designed based on insights obtained from the tackiness test results discussed on the previous section. The cycle time (CT) was fixed at 900 seconds based on both DSC-TGA results which indicated that beyond 900 seconds resulted in no significant outgassing and yielded a comparable degree of cure as previously discussed in Section 4.4.1.

The responses evaluated included both reject yield based on binary GLT outcomes (pass/fail based on the presence or absence of leaks) and quantitative cap shear adhesion strength measurements. The experimental design matrix and corresponding parameter sets for each leg are summarized in Table 2.

Table 1. DoE Experimental Legs with Varying Load Time and Vacuum Off Capsealing Parameters.

Leg No.	LT (s)	VO (s)
1	50	100
2	50	200
3	50	300
4	80	100
5	80	200
6	80	300

The values presented in the table correspond to the time reference at the zero-second mark, defined as the moment

immediately following the complete placement of the caps onto the chase. Specifically, the LT denotes the endpoint at which the ITS plates fully close, signifying the completion of the cap-loading process. The VO time indicates the point relative to the zero-second mark, at which the vacuum system is deactivated and the caps fully attaches to the ceramic header as shown in Fig. 10.

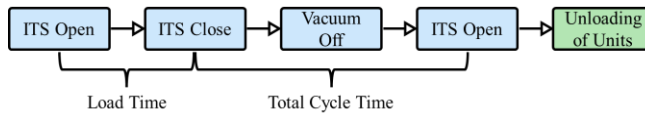


Fig. 10. Sequential Process Flow of the Capsealing Operation Using the ITS Machine.

RSA analysis revealed that both parameters are significant to affect both rejection yield and cap shear strength with p-values of 0.001 and 0.003 respectively. However, no factor interaction was noted indicating that the effect of load time is independent with the timing of vacuum deactivation as exhibited in Fig. 16 in the Appendix. Meanwhile, the cap shear strength values obtained during the experimental trials were consistently and significantly higher than the minimum specification requirement of 25 kgF with recorded measurements ranging from 47.86 kgF to 61.03 kgF, indicating a robust mechanical integrity of the cured capsealing glue under shear stress conditions. Consequently, cap shear strength was deliberately excluded from the response surface optimization analysis to prevent obfuscation of parameter influences and dilution of the statistical sensitivity toward more critical process output specifically the rejection yield, which serves as a more direct indicator of process stability and defectivity. To determine optimum capsealing parameter window, response optimizer was performed targeting zero rejection yield.

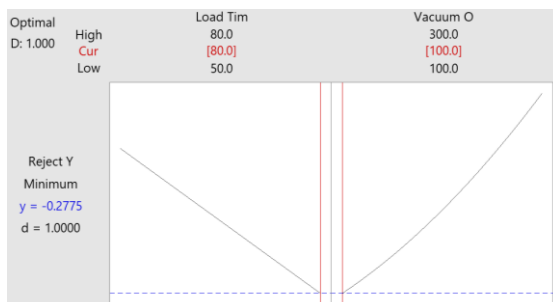


Fig. 11. Optimization Plot of GLT Rejects in Response of Increasing Load Time and Vacuum Off.

Parametric analysis revealed a linear relationship between rejection yield and capsealing parameters. Optimal performance was observed at 80 s load time and 100 s vacuum-off, defining a narrow 20 s window for effective adhesive wetting and void mitigation. The constraint is linked to the adhesive's time-sensitive rheological behavior during vacuum-off, where volatile expulsion may momentarily

disrupt adhesive continuity. Materials with favorable viscoelastic properties can self-level or "self-heal" minor voids prior to cure progression<sup>2,3</sup>. However, the behavior is highly dependent on viscosity and thixotropic recovery as evidenced by tacky tests across different lots. As a result, the process window is not only narrow but also susceptible to further tightening in the presence of material inconsistencies thereby necessitating stringent control over adhesive specifications to ensure reproducibility and yield optimization across production batches. Maintaining load time of 80 s, vacuum-off at 100 s and a cure cycle  $\geq$ 900 s supports sufficient epoxy flow and surface coverage and full crosslinking—ensuring high yield and mechanical reliability.

#### 4.6 Monitoring of Gross Leak Performance

The GLT yield per month was continuously monitored from the moment the optimum parameters from the DoE was implemented in the capsealing process station to check consistency and effectiveness of proposed changes in the parameters.



Fig. 12. Percentage of GLT Rejects by Month Closed Post-Implementation of Optimized Capsealing Parameters With Trendline Overlay.

A significant deviation was observed in April 2025 wherein the rejection yield spiked to 6.03% exceeding the defined acceptance threshold of 3.0%. Detailed failure analysis of the GLT-rejected units revealed prevalent defects such as pinholes and insufficient adhesive coverage suggesting that the existing capsealing parameters were no longer applicable for the glue lots utilized during that production period. To investigate potential material-related causes, tackiness testing was reinitiated to assess deviations in the rheological behavior of the suspect glue lots compared to those previously qualified in earlier production runs as shown in Fig. 17 in the Appendix.

The tackiness evaluation revealed notable differences in the  $\alpha$  and  $\gamma$  phases indicating shifts in both the gelation and vitrification points. Such variations suggest altered thermal and viscoelastic profiles necessitating adjustments in capsealing process parameters particularly in load time and total cure cycle duration. Consequently, the load time was extended to 90 seconds and the total cure cycle to 1200

seconds. The revised conditions proved effective in compensating for the altered rheological behavior of the affected glue lots, restoring process stability and reducing rejection rates. However, the ability of the adjusted parameters to accommodate broader glue lot variability is inherently limited. Extreme rheological deviations may fall outside the compensable range of the current process envelope, rendering such adjustments ineffective for glue lots with substantially different cure kinetics or viscoelastic profiles. In response, a proactive approach was implemented: tackiness testing is now required for both in the outgoing glue batches at the supplier end and the incoming of the company. The strategy enables early detection and characterization of rheological anomalies allowing for timely and informed capsealing parameter adjustments. Although such method does not eliminate the root cause of wide material variability—which remains the responsibility of the adhesive supplier—it provides a practical and cost-effective solution for mitigating defect risks without necessitating additional capital expenditure on advanced incoming quality inspection equipment. The implementation of this rheological monitoring protocol has demonstrated its value in preventing gross GLT rejections and ensuring continued process robustness.

## 5.0 CONCLUSION

The findings showed that the tackiness test method helped revealed critical phase transitions ( $\alpha$ ,  $\beta$ ,  $\gamma$ ) governing adhesive flow and cure behavior, enabling the derivation of optimal process windows. The significance of load time and vacuum-off timing in minimizing GLT rejections was determined through DOE where optimum capsealing parameters of 80-second load time, 100-second vacuum-off point, and 900-second minimum cure duration reduced GLT defects and stabilized process yield. However, post-implementation monitoring revealed the high material variability which could not be covered with the optimized capsealing parameters. Re-emergence of GLT failures prompted further tackiness-based adjustments and the standardization of routine rheological screening for incoming and outgoing glue batches. The proactive strategy effectively mitigated the impact of batch-to-batch inconsistencies without incurring substantial capital investments. Overall, the integration of adhesive rheological profiling with process parameter optimization presents a practical and scalable approach in reducing GLT failures and help maintain hermeticity in ACC packaging. Continuous monitoring on all incoming batches of B-staged cap materials is imperative to sustain long-term process robustness until material variation from the supplier is solved on their end.

## 6.0 RECOMMENDATIONS

It is strongly recommended to evaluate alternative B-stage adhesive materials from other qualified suppliers in the event that material variability remains unresolved with the current source. Substituting with a more consistent formulation may be necessary to ensure process stability and maintain sealing integrity within acceptable reliability requirements.

## 7.0 ACKNOWLEDGMENT

The authors wish to extend their deepest appreciation to the engineers and technicians at the Backend Technologies Competence Center and Assembly Manufacturing Department for their assistance in conducting the experiments, to Failure Analysis & Reliability Department for the execution and provision of necessary tools, tests and support in the experiment, and to the management team of Ampleon Phils. Inc. for their support, which was instrumental in facilitating this research.

## 8.0 REFERENCES

1. J. Joy et al., *Soft Matter*, 19, 2023, 80-89.
2. M. Müller-Pabel et al., *Polym. Test.*, 114, 2022, 107701.
3. M. Bourchak et al., *Adv. Compos. Lett.*, 22(5), 2013, 95-99.
4. J. J. Studer et al., *Compos. - A: Appl. Sci. Manuf.*, 87, 2016, 282-289.
5. B. K. Appelt, P. J. Cook, *Anal. Chem.*, 5, 1984, 57-66.
6. Z. Liu, et al., *J. Therm. Anal. Calorim.*, 109(3), 1984, 1555-1561.

## 9.0 ABOUT THE AUTHORS



**Marty Lorgino D. Pulutan** received the B. S. degree in Applied Physics specializing in Materials Physics from University of the Philippines, Los Baños in 2017 and currently pursuing M. S. degree in Materials Science and Engineering by Research in Mapua University. He has published a total of 11 papers in peer-reviewed journals and international conference proceedings. He is currently a Senior Materials Development Engineer under Back End Technologies Department in Ampleon Philippines, Inc.



**Jelvic D. Fundan** is currently a Sr. Manager for Assembly Process Engineer at Ampleon Manufacturing Philippines handling the Midline and Mechanical Back-End assembly processes. He holds a bachelor's degree in Electronics and Communications Engineering

from the Mapua Institute of Technology. Previously worked as Product/Technical Development Engineer in Amkor Technology Philippines (P3) Flip Chip Ball Grid Array (fcBGA), chip scale package (fcCSP) and Micro-electromechanical systems package (MEMS); and Process Integration Engineer/Product Development Engineer in Taiwan (T3). This gives a total of 17 years of experience in the semiconductor manufacturing industry



**Maria Sandra A. Brucelo**  
received the B. S. degree in  
Business Administration  
specializing in Business  
Management from Trimex  
Colleges, Biñan in 2022. She is  
currently a Materials Development  
Technician under Back End  
Technologies Department in

## Ampleon Philippines, Inc.

## 10.0 APPENDIX

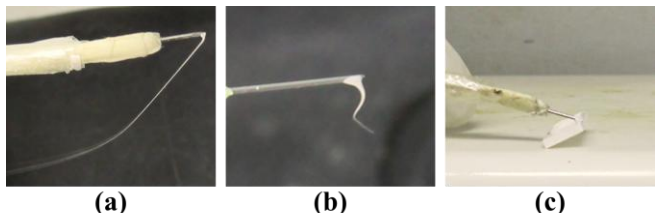


Fig. 13. Representative Images Illustrating Glue Behavior at Various Stages of Tackiness During Probe Testing. (a) Soft stage characterized by high flowability where probing results in the formation of thin, elongated glue filaments. (b) Rubbery stage characterized by reduced flow and elasticity, producing short, thick glue strings that detach cleanly from the cap. (c) Hard stage marked by complete loss of tackiness where the adhesive resists deformation, causing the probe to adhere firmly to the cap with no observable separation.

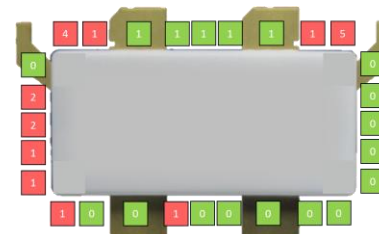


Fig. 14. Defect Mapping of Stretched Glue Defects.

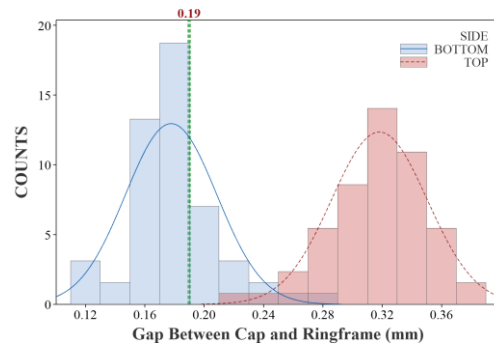


Fig. 15. Histogram of Cap Placement with Respect to Ringframe as Measured on Top and Bottom of the GLT Defective Samples.

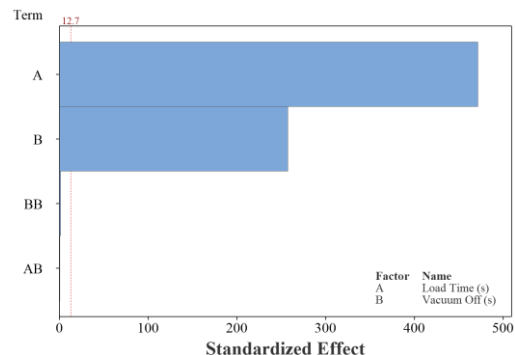


Fig. 16. Pareto Chart of Standardized Effects Showing the Influence of Load Time and Vacuum Off on GLT Yield and Cap Shear Strength.

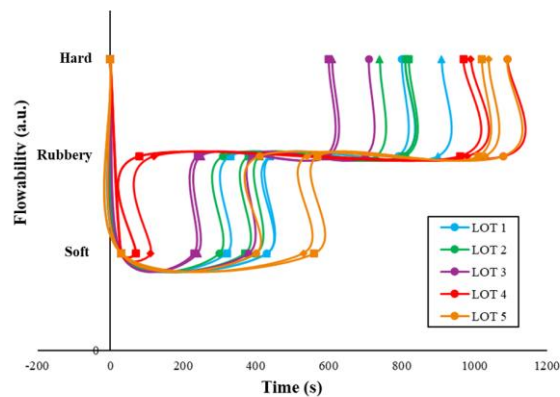


Fig. 17. Flowability Versus Time of B-Staged Cap Samples Randomly Obtained From Two Additional Lots Post-Implementation of Optimized Capsealing Parameters.